

T. Streibel · K. Hafner · F. Mühlberger · T. Adam  
R. Warnecke · R. Zimmermann

## Investigation of NO<sub>x</sub> precursor compounds and other combustion by-products in the primary combustion zone of a waste-incineration plant using on-line, real-time mass spectrometry and Fourier-transform infrared spectrometry (FTIR)

Received: 3 March 2005 / Revised: 29 April 2005 / Accepted: 14 May 2005 / Published online: 21 October 2005  
© Springer-Verlag 2005

**Abstract** On-line analysis of trace and bulk gas compounds in the burning chamber of a waste-incineration plant has been performed, with high temporal resolution, by use of a variety of distinctly different measurement techniques. Time-of-flight mass spectrometry was performed with simultaneous use of three ionization techniques—resonance-enhanced multiphoton ionization (REMPI), single-photon ionization (SPI), and electron-impact ionization (EI). Chemical-ionization mass spectrometry (CIMS), Fourier-transform infrared spectrometry (FTIR), and electrochemical methods were also used. Sampling was conducted by means of a newly developed air-cooled stainless steel lance, to cope with the high temperatures and elevated particle concentrations at the sampling location. Nitrogen species were mainly nitrogen monoxide, ammonia, and hydrogen cyanide (HCN), with a small amount (approximately 0.3%) of aromatic nitrogen compounds. NO, NH<sub>3</sub>, and HCN are the main contributors to the NO<sub>x</sub>-formation process in the postulated fuel–NO reaction scheme dominant at this location. The NO recycling process thereby plays a major role. Changes in plant operating conditions have a noticeable impact

only when the air supply is varied. For example, reduction of oxygen leads to an increase in the HCN fraction of the total nitrogen content and a decrease in the NO fraction, and vice versa.

**Keywords** Mass spectrometry · Photoionization  
On-line · Waste incineration · Nitric oxide

### Introduction

Direct on-line measurement of chemical species in the primary combustion zone of a waste-incineration plant is a challenging issue, because the high-temperature environment causes several problems in sampling and monitoring. With regard to measures for primary reduction of pollutants such as nitric oxides (NO<sub>x</sub>), polycyclic aromatic hydrocarbons (PAH), dioxins, and particulate matter, however, it is important to obtain information about the formation of their precursor compounds which occurs in this environment. Chlorine and sulfur-containing species are also formed in the primary combustion zone, and are responsible for corrosion phenomena in the boiler section. In this work, the practicability of several on-line measurement methods for monitoring gas-phase compounds in the high temperature zone of the burning chamber of a municipal waste-incineration plant are shown by investigation of NO<sub>x</sub> precursor compounds as examples.

Nitric oxides are still a major environmental challenge. These compounds are significant because of several harmful characteristics [1]. First, interaction of NO<sub>x</sub> with ozone is of great importance. The onset of photochemical smog during the summer months is enhanced by nitrogen dioxide via photochemical production of oxygen atoms, which subsequently react with molecular oxygen to yield ozone [2, 3]. Nitric oxides are also part of the catalytic cycle that leads to the decomposition of stratospheric

T. Streibel · K. Hafner · F. Mühlberger · T. Adam  
R. Zimmermann  
Institute of Ecological Chemistry,  
GSF—National Research Centre for Environment and Health,  
85764 Neuherberg, Germany

T. Streibel · T. Adam · R. Zimmermann  
Analytical Chemistry, Institute for Physics,  
University of Augsburg,  
Universitätsstrasse 1, 86159 Augsburg, Germany

R. Zimmermann (✉)  
BIFA GmbH, Am Mittleren Moos 46, 86167 Augsburg, Germany  
E-mail: ralf.zimmermann@gsf.de

R. Warnecke  
GKS Gemeinschaftskraftwerk Schweinfurt GmbH,  
Hafenstrasse 30, 97424 Schweinfurt, Germany

ozone [4].  $\text{NO}_x$  also contribute to the onset of acid rain, although here oxides of sulfur are more important.

The main sources of  $\text{NO}_x$  emissions, accounting for approximately two-thirds of the amount emitted worldwide [5], are combustion processes such as power generation, urban traffic, and, to a much lesser extent, waste incineration. The last of these is, however, interesting because  $\text{NO}_x$  emissions are close to legal standards stipulated by German law ( $200 \text{ mg m}^{-3}$ ) and thus an accompanying reduction process is required. Basically, there are three pathways for formation of the initially emerging nitrogen monoxide, NO:

1. Formation of thermal or Zeldovich NO [6, 7] is strongly dependent on temperature, because of the high activation energy of its rate-determining step (breaking of the strong nitrogen–nitrogen triple bond).
2. Prompt or Fenimore NO [8, 9] is also formed from the nitrogen in air, mainly in a fuel-rich environment. Its contribution to the total amount of NO formed is much smaller than that of thermal NO [9].
3. Formation of fuel NO [10] differs from the other formation pathways in the nature of the nitrogen source. Whereas thermal and prompt NO are derived from nitrogen in the combustion air, fuel NO is formed by oxidation of nitrogen in the fuel. Nitrogen in the fuel is bound to carbon and hydrogen atoms in compounds such as ammonia, pyridine and other amines, and nitriles. This last pathway is the most important in the combustion of solid fuels such as coal, biomass, and waste, and so fuel NO provides the largest fraction of the total amount of nitric oxides formed during combustion processes.

More detailed understanding of the mechanism of formation of nitric oxides from fuel-bound nitrogen continues to be a challenge, even though extensive research on this topic has recently been undertaken, mainly devoted to coal combustion [11–15]. Relatively little is known about other fuels such as biomass and waste and even for coal there are still some unexplained issues. After combustion has started, nitrogen-containing volatile organic compounds are released from the fuel and subsequently oxidized via a complex reaction pattern. The complicated chemistry of these volatile compounds includes oxidation reactions of tar nitrogen, soot nitrogen, aromatic amines, and nitriles. Low-molecular-mass nitrogen compounds such as HCN and  $\text{NH}_3$ , which are released directly from the solid fuel, provide the primary source of nitrogen for conversion into nitrogen monoxide, however [10]. Also, when NO is formed via the fuel NO pathway it can be decomposed by hydrocarbon radicals such as CH and  $\text{CH}_3$ . In this so-called NO-recycling process HCN is reformed and provides a new source of nitrogen for NO formation [10, 16, 17].

This limited knowledge of the detailed chemical and physical processes in the formation of  $\text{NO}_x$  from solid fuels is a problem when designing primary measures for

$\text{NO}_x$  reduction and control, which could be important for facilities such as biomass and waste-incineration plants. To increase our knowledge of the mechanism of formation of nitric oxides, better understanding of the behaviour of volatile precursor compounds during the combustion process is required. Such a task would put special demands on an analytical system, which should enable rapid on-line detection of selected compounds in the combustion zone of waste-incineration plants with sufficient sensitivity.

On-line time-of-flight mass spectrometry (TOFMS) with a combination of different ionization techniques has the potential to meet this requirement [18]. Single-photon ionization (SPI) with vacuum-UV photons of 118-nm wavelength, i.e. a photon energy of 10.49 eV [19–22], enables selective and sensitive ionization, because bulk gases such as nitrogen, oxygen, carbon dioxide, and water are suppressed whereas most organic molecules are ionized. Resonance-enhanced multiphoton ionization (REMPI) [23–27] combines high resolution UV spectroscopy with fast mass spectrometry. Hence, improved selectivity and sensitivity are achieved on a real-time basis. Both SPI and REMPI are, moreover, fragmentation-free ionization techniques, which makes them suitable for analysis of complex mixtures such as combustion gases containing several hundred different organic compounds [28–44]. REMPI–TOFMS was recently used for selective detection of monochlorobenzene, a well-known indicator compound for dioxin concentration, in the flue gas of a waste incinerator [45] and for on-line analysis of target flavour compounds during the coffee-roasting process [46, 47].

The aforementioned bulk components and some inorganic species, for example hydrogen cyanide (HCN), sulfur dioxide ( $\text{SO}_2$ ), and hydrogen sulfide ( $\text{H}_2\text{S}$ ), which are not accessible with either REMPI or SPI can be detected by means of electron-impact ionization (EI).

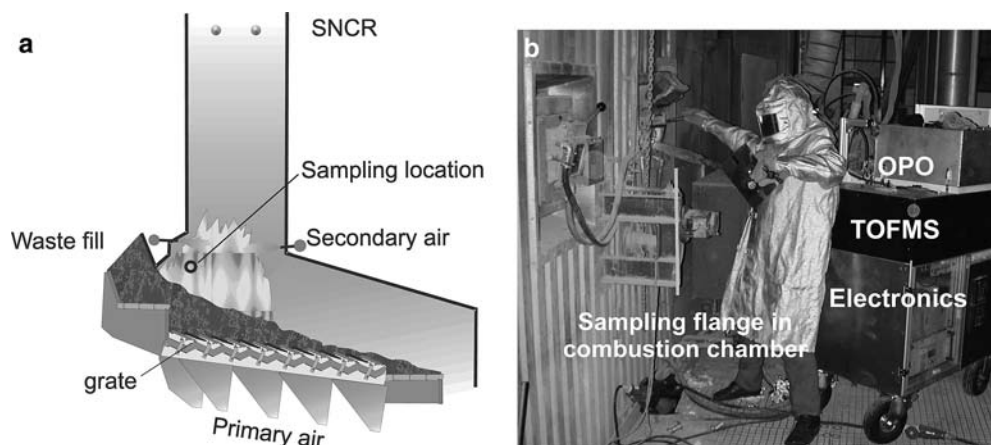
In a parallel paper [48] we report the REMPI spectroscopy of several organic nitrogen compounds known to be potential precursors of nitric oxides, performed in the laboratory using a fine-tuneable stationary UV laser system. The spectroscopic information obtained was subsequently used to measure these compounds in the combustion zone of a waste-incineration plant using a mobile REMPI–TOFMS system. In this study, several different measurement techniques were used to detect and monitor a variety of  $\text{NO}_x$  precursor compounds in the combustion zone of the same WI plant. The effect of selected species on the  $\text{NO}_x$  formation process is discussed on the basis of the results obtained.

---

## Experimental

Measurements in the combustion chamber were conducted at a waste-incineration plant in Bavaria, Germany, with a thermal power of approximately 18.9 MW and a waste capacity of  $8 \text{ t h}^{-1}$ . Flue gas samples were

**Fig. 1** **a** Sampling location directly above the grate in the burning chamber of a waste-incineration plant. **b** Photograph of the sampling location



taken approximately one meter above the grate in the burning chamber. Figure 1a shows a schematic diagram of the sampling location and Fig. 1b a photograph of measurement in progress. Primary air is supplied from underneath the grate, secondary air is injected two meters above the grate, and cooling air is supplied along the walls of the burning chamber. A fraction of the flue gas is recirculated. Under normal combustion conditions  $8 \text{ Nm}^3 \text{ s}^{-1}$  air is supplied. The temperature at the sampling location varied between 1000 and 1250°C.

Because of the high temperatures of the sampled flue gas, a quartz glass lance was inserted inside a high-temperature-resistant stainless steel lance [49], which was placed inside the burning chamber at an ample distance from the wall to avoid edge effects. The air-cooled lance ensures rapid (within 100 ms) cooling of the sample gas to a temperature between 250 and 300°C to reduce the possibility of chemical reactions. The flue gas is pumped

with a flow of  $5 \text{ L min}^{-1}$ . Particles are separated by means of a quartz glass filter and the gas sample is subsequently transported to the analytical devices via deactivated quartz capillaries. The whole sample line is heated to 250°C to avoid condensation and memory effects. A schematic diagram of the sampling set-up is shown in Fig. 2.

The mobile device used to perform on-line SPI/REMPI/EI-TOFMS is described in detail elsewhere [50]. Briefly, an OPO laser system (GWU Lasertechnik, Erfstadt, Germany) is pumped with the third harmonic of a Nd:YAG laser (Surelite-III, Continuum, Santa Clara, CA, USA) to generate UV laser pulses tuneable from 220 to 355 nm, which are used for REMPI. The bandwidth of the UV laser pulses is  $5 \text{ cm}^{-1}$ . A small portion (18%) of the initial 355-nm beam is isolated before entering the OPO system. This part of the beam is focussed into a rare gas cell filled with xenon and produces

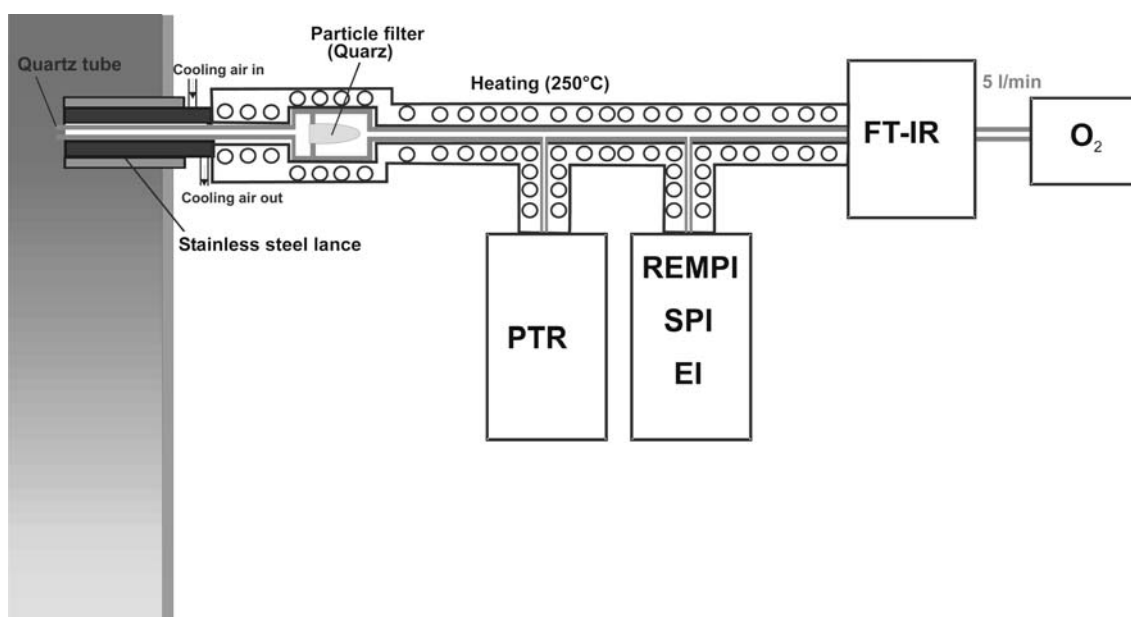


**Fig. 2** Device for sampling in the burning chamber of the waste-incineration plant. All measurement devices are connected to the same sampling line to enable simultaneous measurement. The sampling pump is integrated in the FTIR

the 118-nm VUV light used for SPI by a non-linear frequency-tripling process. The remaining 355-nm beam is separated from the VUV light by means of an MgF<sub>2</sub> lens. Both beams are focussed sharply underneath the stainless steel inlet needle of the sampling line, which consists of a heated, deactivated fused-silica capillary providing an effusive molecular beam.

The molecular ions formed are analyzed with a custom-made reflectron time-of-flight mass spectrometer (Stefan Käs Dorf, Munich, Germany). A mass resolution of  $R_{50\%}$  of 1800  $m/z$  at 92  $m/z$  is achieved. Ion extraction is pulsed, enabling a repetition rate up to 20 kHz. The repeller electrode and the first extraction electrode are at the same potential with opposite polarity, to ensure ground potential for the central ionization region. The effect of the inlet needle on the electrical fields is thus minimized and the needle can be inserted completely into the centre of the ion source, enabling high gas densities and, consequently, more sensitive ionization [41, 51].

Acquisition of the laser ionization TOF mass spectra is performed by a 250 MHz/1 GS/s 128 k transient recorder PC card (model DP 110, Acquiris, Switzerland) at a repetition rate of 5 Hz for either REMPI-TOFMS or SPI-TOFMS, so the respective spectra can be acquired in an alternating manner. The spectra are stored in real-time on the hard disk by a laboratory-written software package (developed with LabView, National Instruments, Austin, TX, USA).

For EI a gateable electron gun is used to produce electrons with a kinetic energy of 23 eV. This low electron energy is advantageous, because the nitrogen signal is reduced owing to the reduced EI cross-section of N<sub>2</sub>. Thus detector saturation and signal disturbance at higher masses are also reduced. The typical time required to generate a time-of-flight spectrum is approximately 20 μs, i.e. when a laser-repetition frequency of 10 Hz is employed; the spectrometer is used only for 200 μs s<sup>-1</sup> to generate SPI and REMPI-TOF mass spectra. The electron gun is therefore operating during the pauses between the ionization laser pulses. By doing this the molecular beam can be characterized by EI-TOFMS at a repetition rate of up to 20 kHz in the respective pauses, i.e. five SPI-TOF mass spectra (8 bit), five REMPI-TOF mass spectra (8 bit), and 19990 EI-TOF mass spectra (1 bit) can be obtained per second. Data acquisition for EI is performed using ion-counting techniques. Because of the high repetition rate and reduced sensitivity, a multichannel analyzer (Fast P7886, Fast ComTec, Munich, Germany) is used. Thus, ten EI-TOF mass spectra composed of 1999 transients can be generated per second (11 bit).

Quantification and calibration, an important issue for analytical techniques, is achieved by use of external standard gases containing relevant analytes in parts-per-million or parts-per-billion volume quantities [52, 53]. The standard gas is either generated according to the “defined leak” principle using diffusion and permeation tubes [54, 55] or commercially available calibration gas

mixtures are used. Limits of detection for selected compounds such as benzene are obtained by use of these methods (see Refs. [50, 56]). A linear relationship between species concentration and signal intensity was ensured over three orders of magnitude [57].

Chemical-ionization mass spectrometry (CI-MS) was performed with a proton-transfer-reaction spectrometer (PTR-MS, Ionicon, Innsbruck, Austria). Either H<sub>3</sub>O<sup>+</sup> or NH<sub>4</sub><sup>+</sup> can be used as primary ion for protonation. These primary ions are generated in the ion source of the mass spectrometer from water vapour and ammonia, respectively, by means of a hollow-cathode discharge. Subsequently, the primary ions are extracted into a short source drift region and pass a venturi type inlet into the long drift tube, where they react with the analyte gas. Ions formed by proton transfer are analyzed with a quadrupole mass spectrometer. Time resolution of the quadrupole mass spectrometer for a whole mass range scan is 10 s. Further details of the device are given elsewhere [58, 59].

Fourier-transform infrared spectra were recorded with a Gasmet DX 4000 interferometer (Ansyco, Karlsruhe, Germany). Maximum resolution is 4 cm<sup>-1</sup> covering a wavelength range between 900 and 4250 cm<sup>-1</sup>. An IR beam incorporating the whole frequency range is divided by means of a half translucent beam splitter. The two partial beams cover different distances and are subject to interference after reflection. Positive and negative interferences are recorded by means of a mercury-cadmium-tellurite detector. By means of Fourier transformation the transmission spectrum is calculated subsequently. Temperature in the FTIR system is held constant at 180°C. The device is able to record a full spectrum every 2 s, to achieve a reasonable signal-to-noise ratio ten consecutive spectra are averaged resulting in a time resolution of 20 s. Quantification is carried out automatically by means of prerecorded reference spectra.

Oxygen was measured using an electrochemical sensor (Testo 300 M; Testo, Lenzkirch, Germany).

## Results and discussion

The fundamental achievement of the laboratory-built SPI/REMPI/EI-TOFMS system is the comprehensive monitoring of chemical species in complex matrices. Figure 3 shows TOF mass spectra from the sampling point (Fig. 1) recorded simultaneously by means of SPI, REMPI at 224 nm, and EI ionization. The waste-incineration plant was operating under normal conditions. For the SPI and REMPI spectra, 100 single spectra are averaged. Between the respective laser pulses flue gas is ionized by a 23-eV electron beam operating at 10 kHz. The spectrum is obtained by averaging 100,000 single transients. By doing so, the spectra in Fig. 3 are recorded within 10 s.

From the spectra depicted the different selectivities and thus different mass spectroscopic information con-

tent become obvious. Combination of the different ionization methods enables simultaneous monitoring of fundamental combustion products present at percentage levels (EI) and of relevant trace chemicals which occur at ppb or ppt levels only (SPI and REMPI).

Aliphatic hydrocarbons such as propyne ( $m/z$  40) and cyclopentadiene ( $m/z$  66), and several aromatic species such as benzene ( $m/z$  78), toluene ( $m/z$  92), and naphthalene ( $m/z$  128) can be detected by means of SPI. Also important is direct analysis of ammonia ( $m/z$  17) and benzonitrile ( $m/z$  103), because both compounds are regarded as intermediates in the  $\text{NO}_x$  formation process, and of  $\text{NO}$  ( $m/z$  30) itself.

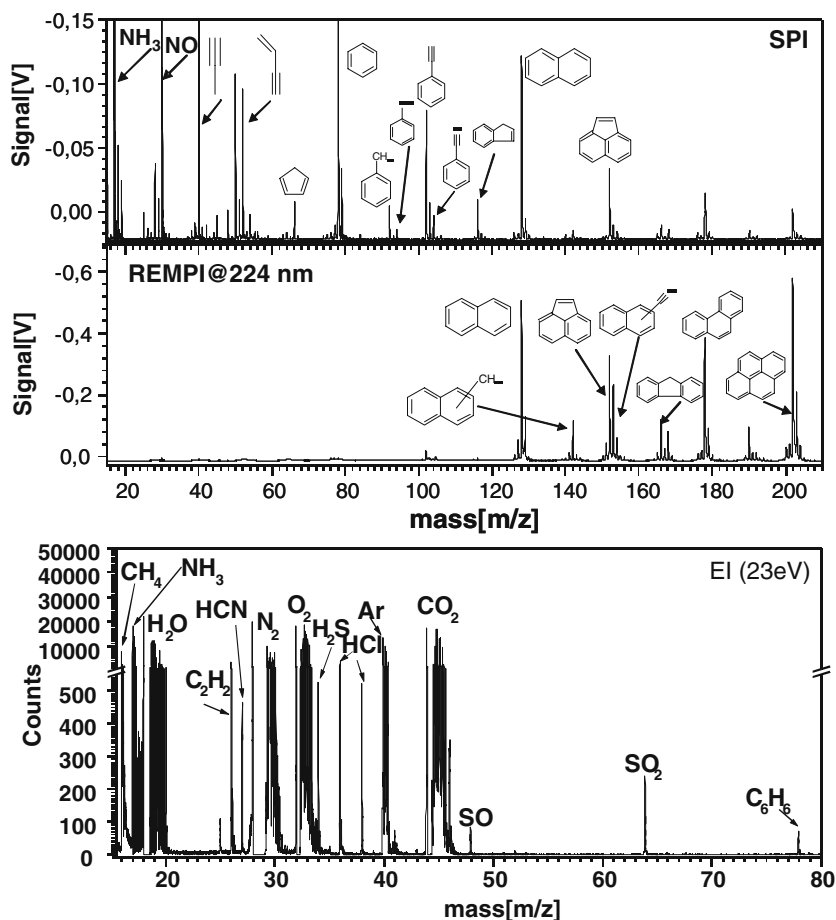
The low abundant PAH are not very accessible with SPI under these measurement conditions, however. Because REMPI is a particularly sensitive means of detection of PAH down to even ppt concentrations [41], the corresponding REMPI spectrum in Fig. 3 shows a variety of further PAH species beyond naphthalene, for example its alkylated derivatives, acenaphthylene ( $m/z$  152), alkylated biphenyls, phenanthrene ( $m/z$  178), and pyrene ( $m/z$  202) with relatively high signal intensities. The chosen wavelength (224 nm), in particular, enables on-line detection of cyanonaphthalene ( $m/z$  153) [56], which is again of special interest in pathways of formation of  $\text{NO}_x$  in the combustion chamber. In principle,

by using other wavelengths for REMPI it is possible to selectively detect other nitrogen-containing species also. By doing so, a given species, e.g. aniline, carbazole, etc., that would otherwise be inaccessible, could be monitored on a real-time basis [48].

Finally, the EI mass spectrum shows the bulk gases (nitrogen, oxygen, argon, and carbon dioxide) and some minor compounds that are suppressed by SPI and REMPI, because their ionization potentials are too high. This category includes methane ( $m/z$  16), acetylene ( $\text{C}_2\text{H}_2$ ,  $m/z$  26), hydrogen cyanide ( $\text{HCN}$ ,  $m/z$  27), hydrogen chloride ( $\text{HCl}$ ,  $m/z$  36) and sulfur dioxide ( $\text{SO}_2$ ,  $m/z$  64), among others.  $\text{HCN}$  is of special interest here, because it is one of the most important precursor compounds of nitric oxides. The benzene signal is relatively low compared with the SPI mass spectrum (with REMPI at 224 nm benzene is not detectable) demonstrating the comparable low cross-section of most organic trace compounds in EI with an electron energy of 23 eV.

Figure 4 shows a typical example of the potential of the SPI/REMPI/EI-TOFMS device for on-line monitoring of selected compounds in the primary combustion chamber. The time profiles in Fig. 4 were recorded over a time span of 20 min. The average temperature at the sampling point during the measurement cycle was

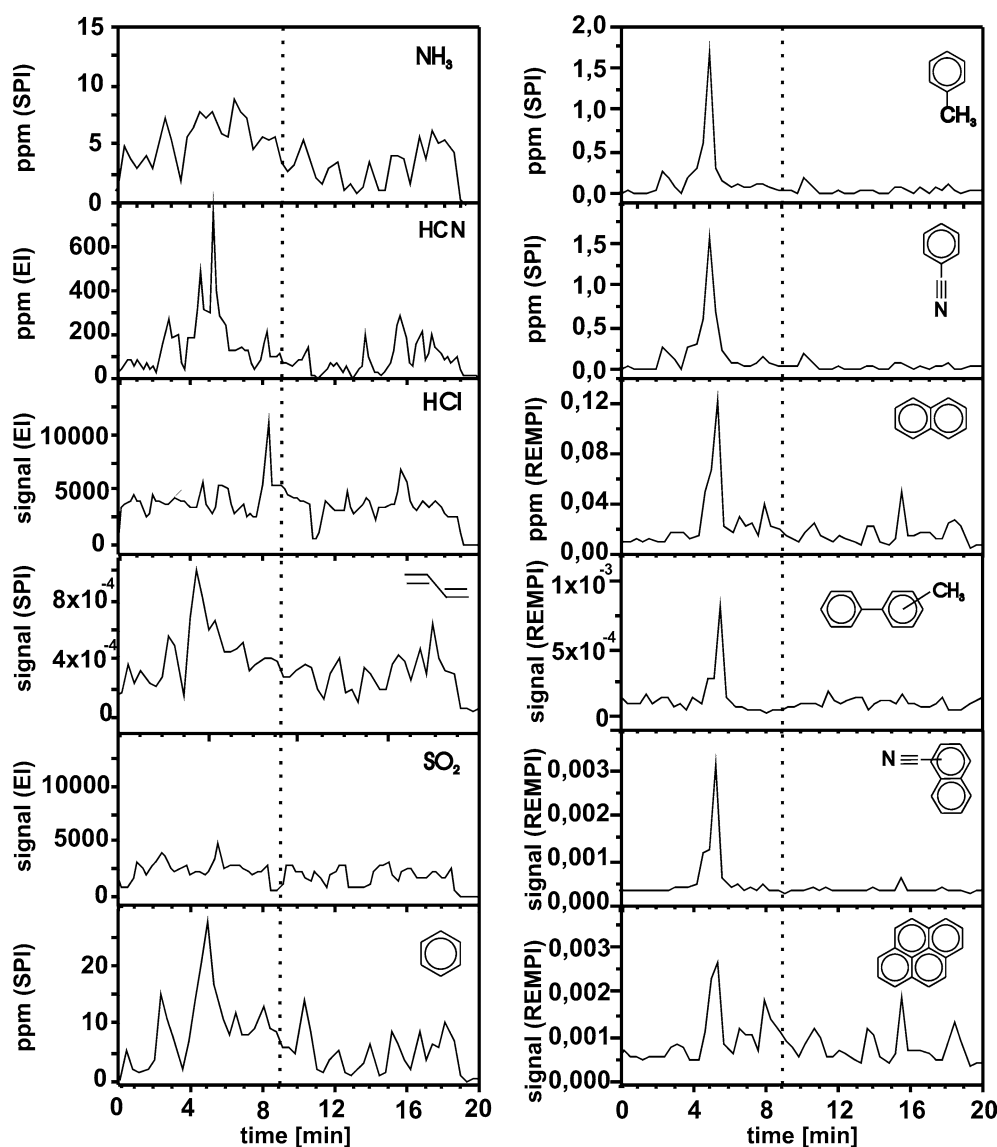
**Fig. 3** Simultaneously recorded on-line SPI at 118 nm, REMPI at 224 nm, and EI-TOF (23 eV) mass spectra of flue gas from the sampling point in the burning chamber of the waste-incineration plant



1200°C. Chemical species are sorted by increasing mass. If appropriate standards were available, quantitative data are given. The dotted line at 9 min measurement time shows the point in time at which the spectra in Fig. 3 are derived. The most striking feature of the time profiles is the increase in concentration at approximately 5 min. The magnitude of this increase varies strongly when different species are examined, however.

In terms of furnishing information about which species affect  $\text{NO}_x$  formation, it is important to detect and monitor as many compounds as possible inside the burning chamber on an on-line real-time basis. The SPI/REMPI/EI-TOFMS measurements were therefore combined with PTR-MS, FTIR, and electrochemical sensing at the same sampling point under normal operating conditions (the experimental set-up is shown in Fig. 2). Combination of these distinct techniques enables comprehensive analysis of the composition of the flue gas.

**Fig. 4** Time profiles of selected compounds in the combustion chamber recorded simultaneously by SPI, REMPI, EI at 224 nm, and EI (23 eV). Compounds are quantified if the corresponding standards were available



Detection of pyridine should exemplify the benefits of applying more than one on-line measurement technique. With SPI-TOFMS, pyridine ( $m/z$  79) interferes with the <sup>13</sup>C peak of benzene. Pyridine is, therefore, not detectable, because of its low concentration—two orders of magnitude below that of benzene. When applying PTR-MS with  $\text{NH}_4^+$  as proton donor, however, benzene is not ionized, because its proton affinity is lower than that of ammonia and its signal vanishes from the mass spectrum, leading to a now undisturbed pyridine mass peak. This is shown in Fig. 5, in which this special selectivity of PTR( $\text{NH}_3$ )-MS for targeted detection of nitrogen compounds is further depicted by direct comparison with PTR( $\text{H}_2\text{O}$ )-MS. The differences between these two protonating media are a consequence of the unequal proton affinities of  $\text{NH}_4^+$  (853.6 kJ mol<sup>-1</sup>) and  $\text{H}_3\text{O}^+$  (690.0 kJ mol<sup>-1</sup>). Most organic species have higher proton affinities than water and are easily protonated after collisions with  $\text{H}_3\text{O}^+$ . Thus, selectivity is relatively low in this instance, and trace compounds such

as aromatic nitrogen-containing species cannot be detected conveniently, because of signal interferences similar to those described above for pyridine in SPI-TOFMS. Because nitrogen compounds often have high proton affinities compared with compounds such as benzene, toluene, phenol, and naphthalene, the latter species are not ionized by  $\text{NH}_4^+$ . Thus, the signals of the aromatic hydrocarbons are suppressed and compounds such as pyrrole, pyridine, aniline, and (iso-)quinoline can be detected selectively with increased sensitivity.

A further advantage of using several detection methods is the opportunity to compare and validate individual results. For example, HCN, a crucial compound in  $\text{NO}_x$  chemistry, is detectable by use of EI-TOFMS, PTR-MS, or FTIR. Figure 6 shows time-resolved trends of HCN concentration from the sampling point recorded simultaneously by the three respective methods. From this figure it becomes obvious that reasonable time resolution is necessary to obtain deeper insight into the temporal characteristics of the concentration of a given species. Because FTIR has only half the time resolution of the other two techniques, short fluctuations in HCN concentration are lost and distinct

maxima are no longer observed. In addition, quantification of FTIR data is complicated by interfering signals from other species. Despite these drawbacks, however, the qualitative course of HCN concentration is satisfactorily met. EI-TOFMS and PTR( $\text{H}_2\text{O}$ )-MS data, in particular, are in good agreement.

Table 1 shows quantitative results from the combustion chamber under normal operating conditions of the plant. Besides the average concentrations for a measurement interval of 10 min, the respective minimum and maximum values and the range which includes 80% of the measurement results are depicted. The chosen measurement techniques for each compound are also listed.

A striking result is the relatively high fluctuation of the oxygen concentration, considering that the data are derived for normal working conditions of the incineration plant. These fluctuations cause comparable variations in the concentration of products of incomplete combustion, for example carbon monoxide and hydrocarbons. Of the aliphatic hydrocarbons, the highest concentrations were observed for methane, followed by acetylene and ethylene. These compounds are well

**Fig. 5** PTR mass spectra in the combustion chamber utilizing  $\text{NH}_4^+$  (above) and  $\text{H}_3\text{O}^+$  (below) as protonating medium

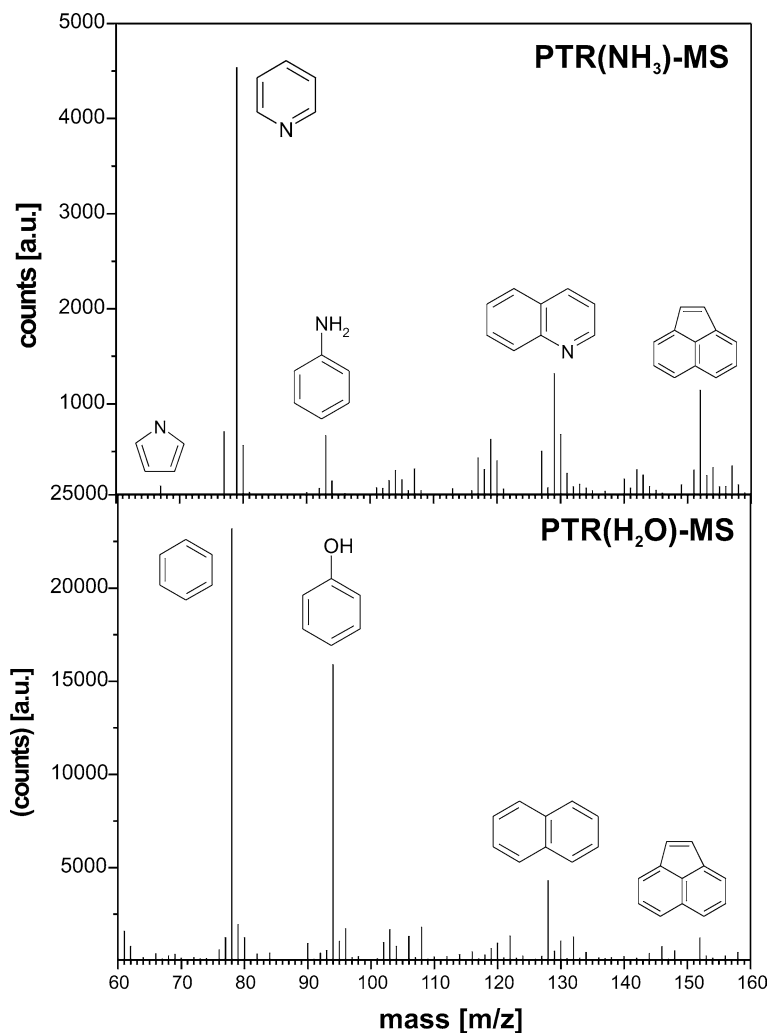
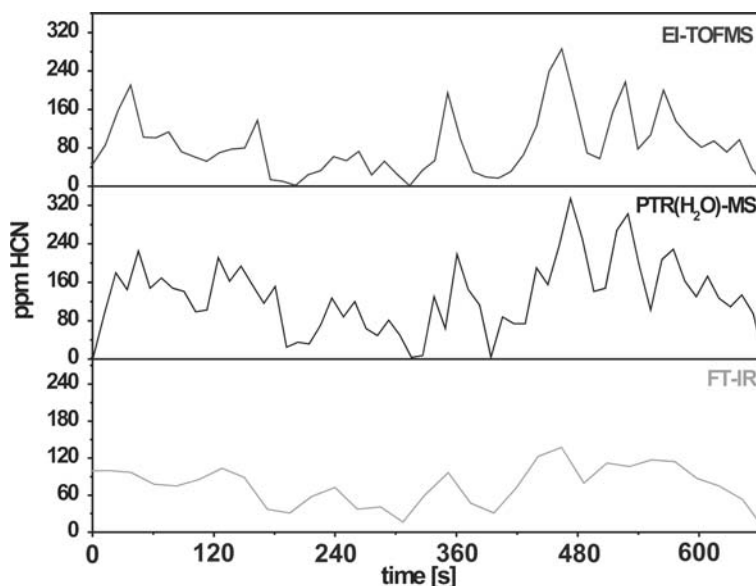


**Fig. 6** Time profiles of HCN concentration simultaneously recorded by means of EI-TOFMS, PTR(H<sub>2</sub>O)-MS, and FTIR



known as the final products of oxidative decomposition of hydrocarbons during the combustion process. The pattern of aromatic hydrocarbons is strongly dominated by benzene and naphthalene, typical indicators of incomplete combustion conditions. The low abundance of alkylated arenes is explicable by the high temperature

at the sampling point, favouring the more stable ring structures without side chains [60]. With regard to nitrogen compounds, besides NO, ammonia and HCN are present at the highest concentrations by far. Nitrogen-containing trace compounds that could be quantified were benzonitrile, cyanonaphthalene, aniline, and

**Table 1** Quantitative data for a variety of chemical species recorded in the combustion chamber

Compound	Average	Minimum	80% Range	Maximum	Detection method
O <sub>2</sub>	1.9%	< LOD	0.5–3.4%	5.5%	Electrochemical
H <sub>2</sub> O	26.9%	20.5%	24.9–29.0%	29.8%	FTIR, EI
CO <sub>2</sub>	10.5%	7.7%	9.1–11.3%	11.5%	FTIR, EI
CO	3.4%	0.6%	1.2–6.2%	10.3%	FTIR
NO	165 ppm	35 ppm	103–207 ppm	237 ppm	SPI, REMPI
NH <sub>3</sub>	279 ppm	150 ppm	206–333 ppm	376 ppm	SPI
HCN	340 ppm	53 ppm	167–559 ppm	898 ppm	EI, FTIR
CH <sub>4</sub>	1167 ppm	390 ppm	777–1480 ppm	1813 ppm	FTIR, EI
Ethane	47 ppm	< LOD	17–79 ppm	119 ppm	FTIR, EI
Ethylene	151 ppm	6 ppm	32–366 ppm	603 ppm	FTIR, EI
Acetylene	696 ppm	120 ppm	334–1172 ppm	1564 ppm	FTIR, EI
Propanediene	2.3 ppm	< LOD	0.8–10.8 ppm	25.5 ppm	SPI
Propylene	2.3 ppm	< LOD	0.1–6.3 ppm	34.5 ppm	SPI
Cyclopentadiene	1.8 ppm	< LOD	0.1–4.4 ppm	19.0 ppm	SPI
Benzene	46 ppm	< LOD	11–86 ppm	142 ppm	SPI, REMPI
Toluene	1.5 ppm	< LOD	0.1–3.5 ppm	16.1 ppm	SPI, REMPI
Phenol	0.4 ppm	< LOD	0.1–0.8 ppm	5.1 ppm	SPI, REMPI
Phenylacetylene	6.8 ppm	< LOD	1.2–14.3 ppm	32.5 ppm	SPI, REMPI
Styrene	1.4 ppm	< LOD	0.1–3.6 ppm	25.0 ppm	SPI, REMPI
Indene	2.2 ppm	< LOD	0.3–5.2 ppm	18.3 ppm	SPI, REMPI
Naphthalene	19.6 ppm	< LOD	3.3–43.5 ppm	89.7 ppm	SPI, REMPI
Acenaphthylene	6.8 ppm	< LOD	1.4–14.0 ppm	29.4 ppm	SPI, REMPI
Fluorene	1.6 ppm	< LOD	0.3–3.8 ppm	13.3 ppm	SPI, REMPI
Phenanthrene	5.8 ppm	< LOD	1.0–13.6 ppm	34.1 ppm	SPI, REMPI
Pyrene	5.1 ppm	< LOD	1.3–10.8 ppm	27.1 ppm	SPI, REMPI
Chrysene	2.0 ppm	< LOD	0.4–4.5 ppm	11.2 ppm	SPI, REMPI
Benzonitrile	1.4 ppm	< LOD	0.2–3.2 ppm	8.5 ppm	SPI, REMPI
Cyanonaphthalene	0.5 ppm	< LOD	0.1–1.0 ppm	2.8 ppm	SPI, REMPI
Pyridine	200 ppb	< LOD	80–320 ppb	1200 ppb	PTR
Aniline	180 ppb	< LOD	60–280 ppb	1050 ppb	REMPI, PTR
Σ aromatics	109 ppm	2.7 ppm	27.5–221 ppm	438.7 ppm	SPI, REMPI
Σ N-aromatics	2.3 ppm	< LOD	0.4–4.8 ppm	13.5 ppm	SPI, REMPI

pyridine.  $\text{NO}_2$  could not be detected, also because of the high temperatures, at which the equilibrium of the reaction  $2\text{NO} + \text{O}_2 \leftrightarrow 2\text{NO}_2$  is entirely shifted to the left side. In total, aromatic nitrogen compounds (average total concentration 2.3 ppm) play only a minor role compared with the averaged sum of all the nitrogen compounds quantified (786 ppm).

Of great importance with regard to  $\text{NO}_x$ -formation processes in the burning chamber are time-resolved profiles of the nitrogen compounds present in the flue gas. Figure 7 shows simultaneous monitoring sequences for these compounds, and those for oxygen and benzene, over a period of 1 h. The data in the figure were obtained during three successive measurement cycles separated by particle filter changes. During the filter change, pure air was detected, indicated by the disappearance of the signals from the nitrogen compounds and an increase in the concentration of oxygen in the respective time profiles. The much higher temporal resolution of the SPI method compared with the other techniques is obvious from the figure; this results in the more polished trends for PTR, FTIR, and electrochemical sensor data. HCN, ammonia, benzene, benzonitrile, and cyanonaphthalene have simi-

lar courses over time, opposite to that for oxygen. Although pyridine and aniline are often in the ranges of their respective detection limits, in the time range between 36 and 38 min after the start of the measurement there are sudden increases in the concentrations of these two species; these correspond to increases in the concentrations of benzene (and other hydrocarbons not shown explicitly here) and HCN and a decrease in the concentration of NO. The NO content is usually approximately 200 ppm and decreases only when oxygen concentrations are very low; a decrease in the time window between 36 and 38 min is, however, especially pronounced. Medium fluctuations of oxygen, HCN, and ammonia do not affect the NO concentration significantly.

This behaviour suggests that NO formation from fuel-derived HCN and  $\text{NH}_3$  is nearly complete at the sampling point. Reduction of NO is then largely caused by the NO recycling process. This is supported by the simultaneous increase in the hydrocarbon content, leading to an increase in the concentrations of CH and  $\text{CH}_3$  radicals and an increase in the concentration of HCN, one of the major products of the NO recycling

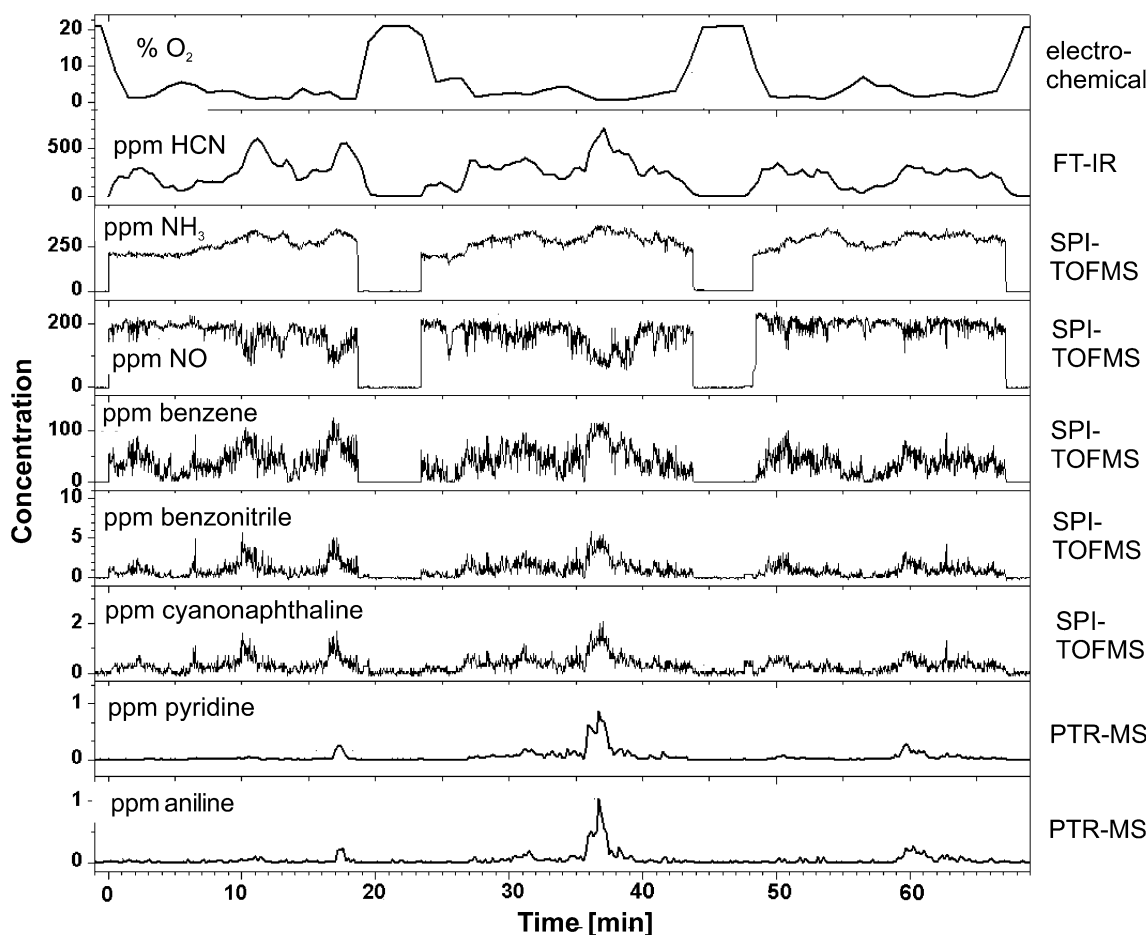


**Fig. 7** Time profiles of nitrogen compounds, oxygen, and benzene at the sampling point. Respective measurement methods are depicted for each compound. Three measurement periods are

shown, separated by changes of particle filter, indicated by a steep increase in the concentration of oxygen and decreases in concentrations of the other species

**Table 2** Deviations of the NO, NH<sub>3</sub>, and HCN fractions of the total nitrogen content from those under normal plant operating conditions

	NO fraction of total N content (%)	NH <sub>3</sub> fraction of total N content (%)	HCN fraction of total N content (%)	Average O <sub>2</sub> concentration (%)
Normal conditions	21.0 ± 2.0	35.5 ± 6.5	43.2 ± 7.4	1.9
R_CA	<b>17.5</b>	33.9	46.0	0.7
R_TA	<b>13.9</b>	35.5	<b>50.7</b>	0.6
R_TP	22.3	36.3	42.2	2.3
I_TA	<b>35.7</b>	32.3	<b>32.0</b>	4.1

Deviations in average oxygen concentration are also displayed. Significant variations are emboldened

reaction scheme. One would also expect a higher ammonia content in the first stages of NO formation, because NH<sub>3</sub> is the primary nitrogen-containing product released from the waste. The concurrent trend of cyanoarenes with HCN and benzene implies their gas-phase formation from these two compounds. Direct release from the waste seems less probable.

In addition to the results obtained from the waste-incineration plant under normal operating conditions, additional measurements were made under intentionally altered combustion conditions. The amount of air feed and its allocation are the easiest conditions to change. Four different operating conditions were investigated:

- reduction of cooling air (R\_CA)
- reduction of total amount of air (R\_TA)
- reduction of total power (R\_TP)
- increase of total air amount (I\_TA)

Table 2 shows the impact of these measures by showing the deviations from normal operating conditions of the amounts of the NO, ammonia, and HCN fractions of the total nitrogen content at the sampling point. In general, the ammonia fraction is not changed significantly by changing the individual operating conditions. Reduction of cooling and total air leads to a decrease in the NO fraction accompanied by an increase in the HCN fraction. This is mainly because the reduced oxygen supply under these conditions leads to increased hydrocarbon formation because of incomplete combustion. Thus, the aforementioned NO recycling process is enhanced, resulting in NO decomposition.

Reduction of the total power does not have a significant impact, or it is not noticeable compared with the fluctuations occurring under normal operating conditions. These fluctuations are mainly caused by the highly inhomogeneous nature of the waste feed. Increasing the total amount of air has a pronounced effect on the pattern, however. A drastic increase in the NO fraction can be observed, accompanied by a simultaneous decrease in the HCN fraction. The increased oxygen concentration results in enhancement of the rate of NO-formation reactions and concurrent suppression of the NO recycling process, because of a decrease in the amounts of hydrocarbon radicals under the more complete combustion conditions.

## Conclusion

Real-time analysis, by mass spectrometry with soft photoionization techniques, of organic nitrogen compounds in the burning chamber of a waste-incineration plant could furnish useful hints enabling more detailed description of the mechanism of formation of fuel NO. At the measurement location selected, nitrogen species consisted mainly of NO, NH<sub>3</sub>, and HCN, with small amounts of aromatic nitrogen compounds. The NO concentration remained nearly constant with time and decreased only when the oxygen content dropped to almost zero. This was accompanied by an increase in HCN and hydrocarbon concentrations, whereas the concentration of ammonia did not change significantly. This suggests a substantial contribution from the NO recycling process. Variation of the working conditions of the plant had a significant impact on the distribution pattern of nitrogen species only when the oxygen content was distinctly changed. Increasing the oxygen content resulted in an increase of the NO fraction and a reduction of the HCN fraction of the total nitrogen content. Overall, no contradictions to proposed fuel NO-formation mechanisms were observed. The postulated opposite trend of NO and ammonia and the parallel course of ammonia and hydrocarbons have been verified by on-line monitoring with high temporal resolution. HCN and ammonia make the principal contributions to NO-formation processes in the location investigated.

SPI/REMPI-TOFMS could conceivably be used for a on-line analysis of a variety of other matrices containing several hundred compounds. New developments of the SPI method, for example VUV photon generation by means of an excimer lamp, could further improve performance with less complexity and expense. Potential future applications could include analysis of toxic target compounds in tobacco smoke and pyrolysis gases.

**Acknowledgements** The work was supported by the German Federal Ministry of Education and Research as part of the HGF strategy funds' project "Primary reduction of NO<sub>x</sub> emissions as an example of optimization of combustion processes in waste-incineration plants".

## References

1. Sillman S (1999) *Atmos Environ* 33:1821–1845
2. Leighton PA (1961) *Photochemistry of air pollution*. Academic Press, New York
3. Rabl A, Eyre N (1998) *Environ Intl* 24:835–850
4. Strand A, Hof O (1995) *Atmos Environ* 30:1291–1303
5. Lee DS, Köhler I, Grobler E, Rohrer F, Sausen R, Gallardo-Klenner L, Olivier JGJ, Dentener FJ, Bouwman AF (1997) *Atmos Environ* 31:1735–1749
6. Zeldovich YB (1946) *Acta Physicochim USSR* 21:577–628
7. Baulch DL, Cobos CJ, Cox AM, Frank P, Haymann G, Just T, Kerr JA, Murrels T, Pilling MJ, Twe J, Walker RW, Warnatz J (1991) Supplement I. *J Phys Chem Ref Data* 22:847
8. Fenimore CP (1976) *Combust Flame* 26:249–256
9. Hayhurst AN, Vince IM (1980) *Prog Energy Combust Sci* 6:35–51
10. Glarborg P, Jensen AD, Johnsson JE (2003) *Prog Energy Combust Sci* 29:89–113
11. Visona SP, Stanmore BR (1996) *Combust Flame* 105:92–103
12. Glarborg P, Alzueta MU, Dam-Johansen K, Miller JA (1998) *Combust Flame* 115:1–27
13. Molina A, Edings EG, Pershing DW, Sarofim AF (2000) *Prog Energy Combust Sci* 26:507–531
14. Wu Z, Sugimoto Y, Kawashima H (2001) *Fuel* 80:251–254
15. Taniguchi M, Yamamoto K, Kobayashi H, Kiyama K (2002) *Fuel* 81:363–371
16. Dagaut P, Luche J, Cathonnet M (2000) *Combust Flame* 121:651–661
17. Cant NW, Cowan AD, Liu IOY, Satsuma A (1999) *Catal Today* 54:473–482
18. Boesl U, Weinkauff R, Weickhardt C, Schlag EW (1994) *Intl J Mass Spectrom Ion Proc* 131:87–124
19. Miller JC, Compton RN (1982) *J Chem Phys* 76(8):3967–3973
20. Pallix JB, Schühle U, Becker CH, Huestis DL (1989) *Anal Chem* 61:805–811
21. Butcher DJ (1999) *Microchem J* 62:354–362
22. Tonokura K, Nakamura T, Koshi M (2003) *Anal Sci* 19:1109–1113
23. Boesl U, Neusser HJ, Schlag EW (1978) *Z Naturforsch* 33A:1546–1548
24. Tembreull R, Sin CH, Pang HM, Lubman DM (1985) *Anal Chem* 57:2911–2917
25. Hager JW, Wallace SC (1988) *Anal Chem* 60:5–10
26. Lubman DM (1990) *Lasers and mass spectrometry*. Oxford University Press, New York
27. Boesl U, Zimmermann R, Weickhardt C, Lenoir D, Schramm K-W, Kettrup A, Schlag EW (1994) *Chemosphere* 29:1429–1440
28. Becker CH (1991) *Fresenius J Anal Chem* 341:3–6
29. Butcher DJ, Goeringer DE, Hurst GB (1999) *Anal Chem* 71:489–496
30. Kornienko O, Ada ET, Tinka J, Wijesundara MJB, Hanley L (1998) *Anal Chem* 70:1208–1213
31. Materer N, Goodman RS, Leone SR (1997) *J Vac Sci Technol A* 15(4):2134–2142
32. McEnally CS, Pfefferle LD, Mohammed RK, Smooke MD, Colket MB (1999) *Anal Chem* 71:364–372
33. Shi YJ, Hu XK, Mao DM, Dimov SS, Lipson RH (1998) *Anal Chem* 70:4534–4539
34. Steenvoorden RJJM, Kistemaker PG, Vries AE, Michalak L, Nibbering NMM (1991) *Intl J Mass Spectrom Ion Proc* 107:475–489
35. Trevor JL, Hanly L, Lykke KR (1997) *Rapid Commun Mass Sp* 11:587–589
36. Vries MS, Hunziker HE (1997) *J Photochem Photobiol A* 106:31–36
37. Zoller DL, Sum ST, Johnston MV (1999) *Anal Chem* 71:866–872
38. Zimmermann R, Heger HJ, Kettrup A, Boesl U (1997) *Rapid Commun Mass Sp* 11:1095–1102
39. Zimmermann R, Heger HJ, Kettrup A (1999) *Fresenius J Anal Chem* 363:720–730
40. Zimmermann R, Dorfner R, Kettrup A (1999) *J Anal Appl Pyrol* 49:257–266
41. Heger HJ, Zimmermann R, Dorfner R, Beckmann M, Griebel H, Kettrup A, Boesl U (1999) *Anal Chem* 71:46–57
42. Oser H, Thanner R, Grotheer H-H (1996) *Combust Sci Technol* 116–117:567–582
43. Grotheer H-H, Nomayo M, Pokorny H, Thanner R, Gullett BK (2001) *Trends Appl Spec* 3:181–206
44. Oudejans L, Touati A, Gullett BK (2004) *Anal Chem* 76:2517–2524
45. Heger HJ, Zimmermann R, Blumenstock M, Kettrup A (2001) *Chemosphere* 42:691–696
46. Dorfner R, Ferge T, Kettrup A, Zimmermann R, Yeretizian C (2003) *J Agric Food Chem* 51:5768–5773
47. Dorfner R, Ferge T, Yeretizian C, Kettrup A, Zimmermann R (2004) *Anal Chem* 76:1386–1402
48. Streibel T, Hafner K, Mühlberger F, Adam T, Zimmermann R (2005) *Appl Spec*, accepted for publication
49. Mühlberger F (2003) *Entwicklung von on-line-Analyseverfahren auf Basis der Einphotonenionisations-Massenspektrometrie*. PhD Thesis, Technische Universität München
50. Mühlberger F, Hafner K, Kaesdorf S, Ferge T, Zimmermann R (2004) *Anal Chem* 76:6753–6762
51. Harris S (1969) *Proc IEEE* 57:2096–2113
52. Mühlberger F, Zimmermann R, Kettrup A (2001) *Anal Chem* 73:3590–3604
53. Gittins CM, Castaldi MJ, Senkan SM, Rohlfing EA (1997) *Anal Chem* 69:286–293
54. Steenvoorden RJJM, Hage ERE, Boon JJ, Kistemaker PG, Weeding TL (1994) *Org Mass Spec* 29:78–84
55. Nir E, Hunziker HE, Vries MS (1999) *Anal Chem* 71:1674–1678
56. Hafner K (2004) *Untersuchungen zur Bildung brennstoffabhängiger Stickoxide bei der Abfallverbrennung mittels on-line analytischer Messmethoden*. PhD Thesis, Technische Universität München
57. Mitschke S, Adam T, Streibel T, Baker RR, Zimmermann R (2005) *Anal Chem* 77:2288–2296
58. Lindinger W, Hansel A, Jordan A (1998) *Intl J Mass Spectrom Ion Proc* 173:191–241
59. Lindinger W, Hirber J, Paretzke H (1993) *Intl J Mass Spectrom Ion Proc* 129: 79–88
60. Cao L, Mühlberger F, Adam T, Streibel T, Wang HZ, Kettrup A, Zimmermann R (2003) *Anal Chem* 75:5639–5645